Journal of Analytical and Applied Pyrolysis 159 (2021) 105337

Contents lists available at ScienceDirect

Journal of Analytical and Applied Pyrolysis

journal homepage: www.elsevier.com/locate/jaap

Importance of pyrolysis temperature and pressure in the concentration of polycyclic aromatic hydrocarbons in wood waste-derived biochars

Gianluca Greco [a,*], María Videgain [b], Christian Di Stasi [a], Elisabet Pires [c], Joan J. Manyà [a,*]

[a] Aragón Institute of Engineering Research (I3A), Thermochemical Processes Group, University of Zaragoza, Escuela Politécnica Superior, crta. Cuarte s/n, Huesca, E-22071, Spain
[b] Escuela Politécnica Superior, University of Zaragoza, crta. Cuarte s/n, Huesca, E-22071, Spain
[c] Departamento de Química Orgánica ISQCH, Facultad de Ciencias, Universidad de Zaragoza-CSIC, Pedro Cerbuna 12, Zaragoza, 50009, Spain

ARTICLE INFO

Keywords:
Biochar
Slow pyrolysis
Pressure
Untreated wood waste
PAH assessment
Phytotoxicity

ABSTRACT

Biochar addition to soil can lead to potential environmental risks due to its content of polycyclic aromatic hydrocarbons (PAHs). Until now, previous research focused on assessing the influence of pyrolysis peak temperature and feedstock on the formation and evolution of PAHs. Nevertheless, the effects of other important process parameters —such as pressure, gas residence time, and type of carrier gas— have not been comprehensively explored. To fill this gap, a 2-level full factorial design of experiments was conducted to assess the influence of the above-mentioned parameters on the pyrolysis behavior of an untreated wood waste as well as the properties of resulting biochars, including their PAHs contents. Results showed that the highest production of PAHs was reached at lower peak temperatures, whereas an increase in temperature led to a substantial reduction of the final PAHs content. An increased pressure also resulted in a marked decrease in PAHs, probably as a consequence of the higher carrier gas flow rates used under pressurized conditions, which could inhibit the generation of PAHs by condensation and polymerization. The outstanding results obtained from the phytotoxicity assessment for three plant species (barley, watercress, and basil) suggest that PAHs were not the major responsible for the observed short-term phytotoxic effects of biochars, since a considerable part of the phytotoxic compounds in biochar can be removed by a simple water washing step.

1. Introduction

Biochar is widely recognized as a potential soil amendment due to its unique properties, such as high stability, high nutrients content, alkalinity, and relatively high porosity [1]. Although the research in the field of biochar has been very intensive in the last years, a better understanding of its role in agricultural and environmental practices is still needed. Biochar addition to soil also entails potential environmental risks due to its content of polycyclic aromatic hydrocarbons (PAHs). Being the largest group of carcinogenic, teratogenic and mutagenic compounds, PAHs are nowadays recognized as priority pollutants [2]. Allowed levels of PAHs in biochar for soil applications have been proposed in the last years, defining basic- and premium-grade biochars: below 12 and 4 mg kg^{-1}, respectively, according to the European Biochar Certificate [3]; and below 20 and 6 mg kg^{-1}, respectively, in line with the International Biochar Initiative [4].

PAHs are highly condensed aromatic structures produced during the pyrolysis process [5]. Their final concentrations in the produced biochar —which typically range from less than 0.1 to over 10,000 mg kg^{-1} [6]— depend on both the pyrolysis operating conditions (especially pyrolysis peak temperature) and biomass feedstock [7]. However, the effect of pyrolysis peak temperature on the production and distribution of PAHs within the resulting biochar is still unclear, in light of the apparently contradictory findings available in the literature [8–10]. It is known that aromatization, cyclization, dehydrogenation and dealkylation are the main reactions involved in PAHs formation at relatively low peak temperatures [11] (i.e., below 500 °C), whereas a further recombination of reactive radicals occurs when more severe conditions are applied, leading to the formation of more condensed aromatic structures [12].

In addition to pyrolysis peak temperature, the gas residence time can also markedly affect the final PAHs content in biochar. Typically, its increase results in a prolonged contact between the solid and gas phases, leading to a further decomposition of the tarry vapors onto the solid carbonaceous matrix through secondary reactions such as condensation, repolymerization and thermal cracking [13]. In other words, longer gas

* Corresponding authors.
E-mail addresses: greco@unizar.es (G. Greco), joanjoma@unizar.es (J.J. Manyà).

https://doi.org/10.1016/j.jaap.2021.105337
Received 20 July 2021; Received in revised form 31 August 2021; Accepted 24 September 2021
Available online 28 September 2021

Nomenclature

Abbreviations of 16 EPA PAHs

ANA	Acenaphthene
ANT	Anthracene
&%Annotation-xml.content;	Acenaphthylene
BaA	Benzo[a]anthracene
BaP	Benzo[a]pyrene
BbF	Benzo[b]fluoranthene
BkF	Benzo[k]fluoranthene
BPE	Benzo[ghi]perylene
CHR	Chrysene
DBA	Dibenz[a,h]anthracene
FLT	Fluoranthene
FLU	Fluorene
IPY	Indeno[1,2,3,-cd]pyrene
NAP	Naphthalene
PHE	Phenanthrene
PYR	Pyrene

Variables

CO_2	CO_2 content in the pyrolysis carrier gas (vol. %)
G	Germination percentage
GI	Germination index (%)
L	Average root length (mm)
P	Absolute pressure during pyrolysis (MPa)
S_{BET}	Specific surface area according to the BET model ($m^2\ g^{-1}$)
T	Pyrolysis peak temperature (°C)
τ	Gas residence time (s)
V_{ultra}	Volume of ultra-micropores ($cm^3\ g^{-1}$)
x_{FC}	Fixed-carbon content (wt. %)
y_{char}	Yield of char (mass fraction, daf basis)
y_{FC}	Fixed-carbon yield (mass fraction)
y_{gas}	Yield of produced gas (mass fraction, daf basis)
y_{org}	Yield of condensable organic compounds (mass fraction, daf basis)
y_{wat}	Yield of produced water (mass fraction, daf basis)

Acronyms

daf	*Dry- and ash-free basis*
db	*Dry basis*
TTEC	Total toxic equivalent concentrations ($\mu g\ kg^{-1}$ biochar, db)

Subscript

w	Washed biochar samples

residences times could result in biochars with higher PAHs contents, since PAHs are predominantly synthesized in the gas phase [5]. In line with this, Madej et al. [14] observed that using relatively high carrier gas (N_2) flow rates during the pyrolysis of several biomass sources led to biochars with low PAHs contents (less than 1.5 mg kg^{-1}), regardless of the peak temperature used.

On the other hand, the effect of the absolute pressure on the production and distribution of PAHs has been much less explored. Since it was found that an increased pressure can significantly affect the pyrolysis process —leading to higher yields of gas at the expense of condensable organic products [15–19]—, a certain influence of this process parameter on the PAHs contents of produced biochars can be expected. At this point, it should be emphasized that pressurized pyrolysis coupled with CO_2-containing flue gas recirculation appears as a promising approach in terms of energy efficiency [16]. The presence of CO_2 in the pyrolysis atmosphere was previously tested in different works [15,16,20]. For instance, Azuara et al. [20] analyzed the effects of absolute pressure coupled with a CO_2 pyrolysis atmosphere during the slow pyrolysis of vine shoot biomass, demonstrating that the switch from N_2 to CO_2 did not affect neither the carbonization efficiency nor the properties of resulting biochar. In addition, under a CO_2 atmosphere, the yield of CO notably increased at the expense of the CO_2 yield, leading to the production of a more refined gas product, with a higher energy content. In light of these previous findings, which clearly appeared to be very appealing from an energy point of view, the role played by the content of CO_2 in the carrier gas in the genesis of PAHs results to be very interesting to assess.

It is estimated that the countries of the EU generate 50 million cubic meters of wood waste (WW) each year [21]. WW can be considered a valuable material, due to its potential for both recycling (e.g., particleboard) and energy recovery. However, WW could contain chemical impurities, such as heavy metals and persistent organic pollutants, including PAHs, which could be present in adhesives used in panels production [22]. Hence, and in order to produce high-quality biochars (with low PAHs levels), using untreated wood waste as precursor is encouraged.

Keeping in mind all the considerations given above, the present work aims at assessing the influence of four pyrolysis process parameters (peak temperature, absolute pressure, gas residence time, and content of CO_2 in the carrier gas) on the pyrolysis behavior and physicochemical properties of resulting biochars, with a special emphasis on their PAHs contents. Phytotoxicity of WW-derived biochars was also evaluated through germination tests for different seeds (i.e., barley, watercress, and basil). To the best of our knowledge, the present study is among the first ones to assess the influence of a high number of process-related variables (not only peak temperature, which has been the most analyzed parameter so far) on the potential hazard of WW-derived biochar utilization.

2. Experimental section

2.1. Biomass feedstock

An untreated wood waste, which was basically a mixture of sawdust from sawmills and wood from used pallets and crates, was provided from a Belgian wood recycling company. The used WW, with a particle size in the range of 0.30–4.0 mm, was directly pyrolyzed without any preliminary treatment. Proximate analyses were performed in quadruplicate according to ASTM standards for moisture, volatile matter, and ash contents. Ultimate analyses were carried out in triplicate using a CHN628 elemental analyzer (Leco, USA). X-Ray Fluorescence (XRF) spectroscopy analysis (using an ADVANT'XP + XRF spectrometer from Thermo ARL, Switzerland) was also conducted to determine the inorganic constituents of the biomass ash. The procedure employed to determine the main constituents of WW (hemicelluloses, cellulose, lignin, and extractives) is reported in detail in a previous work [16].

2.2. Production and characterization of WW-derived biochars

The bench-scale fixed-bed pyrolysis unit used for biochar production was already described in an earlier study [15]. Pyrolysis experiments were performed by varying the peak temperature between 400 and 550 °C, whereas the ranges of absolute pressure and gas residence time were 0.2–0.9 MPa and 100–200 s, respectively. Moreover, the composition of the carrier gas varied from pure N_2 to a binary mixture of 60:40 v/v of CO_2/N_2. The initial mass of WW was 400 g and the mean heating rate and the soaking time (at the peak temperature) were kept constant at 5 °C min^{-1} and 1 h, respectively. More details concerning the experimental

device and procedure are available in Appendix A.

The mass yields of biochar (y_{char}), produced gas (y_{gas}), organic condensable products (y_{org}) and produced water (y_{wat}) were calculated in a dry and ash-free (daf) basis. Produced biochars were characterized by proximate analysis and ultimate analyses using the same procedures as described above. The fixed-carbon yield (y_{FC}), which corresponds to the fraction of organic matter initially present in the biomass feedstock and converted into fixed carbon, was taken as a measure of carbonization efficiency.

Given the highly ultra-microporous structure of biochars, CO_2 adsorption isotherms at 0 °C were measured using an ASAP 2020 gas sorption analyzer (Micromeritics, USA). Approximately 120 mg of each sample were firstly degassed under dynamic conditions at 150 °C until constant weight was reached. From the obtained isotherms, the BET specific surface areas (S_{BET}) and the ultra-micropore volumes (V_{ultra}, pore size lower than 0.7 nm) were determined. For V_{ultra}, Grand Canonical Monte Carlo (GCMC) simulations for carbon slit-shaped pores were used.

The pH of biochars was measured in deionized water at a ratio of 1:10 (w/v) using a pH meter (SensION + pH3 from Hach, USA). For comparison purposes, pH of raw and water-washed biochars was measured. A large excess of distilled water (50 mL per g of biochar) was used for washing. The resulting mixture was gently stirred for 2 h at 300 rpm. The washed biochar particles were then separated by vacuum filtration and dried at 105 °C overnight.

2.3. PAHs contents in biochars

In line with the methodology described by De la Rosa et al. [23], 2 g of dried biochar underwent a Soxhlet extraction using 200 mL of toluene throughout 24 h without any clean-up treatment. The obtained extracts were concentrated to 1 − 2 mL by means of a rotary vacuum evaporator (R-210, Buchi, Switzerland). Prior to concentration, the biochar samples were spiked with 10 μL of toluene containing 400 ng of a PAH deuterated internal standard mix in order to detect any possible loss of analyte during sample preparation. The analysis of the 16 PAHs prioritized by the US EPA in the resulting extracts was performed using a 6890 GC coupled with a 5973i MS detector (Agilent, USA). More details on the procedure adopted to measure PAHs are available in Appendix A. The total toxic equivalent concentrations (*TTEC*) related to the carcinogenic risk assessment for each biochar sample was then calculated according to the procedure described by Dat and Chang [24].

2.4. Germination tests

Phytotoxicity tests were carried out in order to assess the hazard of employing WW-derived biochar as soil amendment. The procedure consisted of the incubation of 10 seeds (of barley, watercress, or basil) in 5 mL of an aqueous solution containing 0.5 g of biochar poured in a Petri dish over a sterile filter paper. All the samples were then covered and stored in an oven at 25 °C for 72 h. The root length of germinated seeds was measured using a Vernier caliper and the average values were calculated for each sample. According to Liang et al. [25], the germination index (*GI*) was calculated as follows:

$$GI = \frac{G}{G_0}\frac{L}{L_0}100 \quad (1)$$

where G and L are the germination percentage and average root length, respectively. G_0 and L_0 refer to the control condition (i.e., Petri dish with 5 mL of deionized water).

2.5. Statistical approach

An unreplicated 2-level full factorial design was adopted to evaluate the effects of the four factors assessed —peak temperature (T, 400 and 550 °C), absolute pressure (P, 0.2 and 0.9 MPa), gas residence time (τ, 100 and 200 s), and CO_2 content in the carrier gas (*CO2*, 0 and 60 vol. %). Three replicates at the center point (475 °C, 0.55 MPa, 150 s and 30:70 v/v of CO_2/N_2) were carried out to estimate the experimental error and the overall curvature effect [26]. The structure of the regression model for a given response variable —using normalized values for factors (x) in the range from –1 to 1— was as follows:

$$\hat{y} = \beta_0 + \sum_{i=1}^{4}\beta_i x_i + \sum_{i=1}^{4}\sum_{j=1}^{4}\beta_{i,j}x_i x_j + \sum_{i=1}^{4}\sum_{j=1}^{4}\sum_{k=1}^{4}\beta_{i,j,k}x_i x_j x_k \quad (2)$$

where β_0, β_i, β_{ij}, β_{ijk} are the intercept, linear, 2-way interaction and 3-way interaction coefficients, respectively. All the statistical calculations were conducted using Minitab software (v17).

3. Results and discussion

3.1. Pyrolysis behavior

Results from proximate, ultimate, and XRF analyses —as well as lignocellulosic constituents— related to the WW feedstock are listed in Table 1. The relatively low content of nitrogen confirms the absence of nitrogen adhesives and/or melamine [27]. However, titanium was found in a non-negligible amount (67.0 mg kg^{-1} db), probably due to the marginal presence of TiO_2-based paint pigments. In any case, the content of Ti was considerably lower than those reported for treated waste woods (e.g., 1600 [27] and 2140 mg kg^{-1} db [28]).

From the analysis of the obtained pyrolysis mass loss curves and temperature profiles, it can be underlined that similar conclusions to those previously reported for wheat straw [16] can be drawn. In this regard, an increased pressure enhanced the kinetics of the reactions involved in the overall devolatilization process. For WW, however, kinetics was improved to a lesser extent in comparison with those corresponding to wheat straw, probably due to the lower hemicelluloses content in the WW feedstock, which is the first biomass fraction to

Table 1
Lignocellulosic composition, proximate, ultimate and XRF analyses of WW.

Component (wt. %)	
Hemicelluloses	18.0 ± 0.7
Cellulose	52.3 ± 0.3
Lignin	28.9 ± 0.2
Extractives	0.80 ± 0.2
Proximate (wt. %)	
Ash	0.36 ± 0.05
Moisture	7.61 ± 0.02
Volatile matter	80.2 ± 0.21
Fixed carbon	11.9 ± 0.23
Ultimate (wt. % in daf basis)	
C	45.9 ± 0.07
H	6.36 ± 0.02
N	0.36 ± 0.01
O (*by difference*)	47.0
Inorganic matter (mg kg^{-1} in dry basis)	
Ca	400.0 ± 18
K	113.4 ± 5.8
Ti	67.0 ± 3.2
Fe	67.0 ± 3.2
Si	53.3 ± 2.5
S (inorganic)	43.2 ± 2.2
Mn	40.0 ± 2.2
Cl (inorganic)	39.6 ± 1.8
Mg	23.8 ± 2.3
Al	22.0 ± 1.1
Pb	21.9 ± 1.5
Zn	11.9 ± 0.7
Sn	10.6 ± 0.8

thermally decompose. Further details on this study are available in Appendix A.

The mass balance closures and the distributions of the pyrolysis products obtained for each experiment are listed in Table 2. The error in the mass-balance closure (which ranged from 78 % to 92 %) was attributed to the difficulty in accurately determining the mass of produced gas, especially at high carrier gas flow rates. The outcomes from the statistical analyses for the response variables related to the yields of pyrolysis products are given in Table A.2.

Fig. 1 displays the normal probability plots of the standardized effects on the yields of biochar, gas, condensable organics, and produced water. As expected and in line with previous studies [29–31], an increased peak temperature resulted in a lower yield of biochar, due to the higher extent of devolatilization at temperatures higher than 400 °C. To a much lesser extent than peak temperature, using a CO_2-containing carrier gas also led to a decreased yield of biochar. This can probably be ascribed to a slight gasification of the carbonaceous matrix with CO_2. In contrast, an increase in the absolute pressure resulted in a slight increase in y_{char}, probably as a result of the major extent of the secondary charring reactions. At this point, it should be pointed out that apparently contradictory results with regard to the effect of pressure on the yield of char have been reported. For instance, Melligan et al. [32] did not observe any significant correlation, whereas Manyà et al. even reported a slight negative effect of the absolute pressure in some studies [33,34]. A reason for this dissimilarity could be the fact that the present study incorporates the gas residence time as a parametric factor. This allowed us to separate properly the pure effects of the absolute pressure and the gas residence time. Another reason could be the influence of the processed biomass feedstock, especially in terms of biomass constituents and inorganic matter content and composition.

As can also be seen in Fig. 1, higher levels of pressure considerably promoted the yield of produced gas at the expense of the overall condensable products (y_{org} and y_{wat}). This could be explained by an enhancement of secondary reactions at pressurized conditions, with a consequent further consumption of volatiles and a higher release of non-condensable gases [16]. In fact, and as can be deduced from Fig. 1d, the main effect of the absolute pressure on y_{gas} was notably higher than that of the peak temperature. The observed decrease in the yield of produced water (see Fig. 1c) could probably be due to an enhancement of both water gas shift and reforming (of intermediate volatiles) reactions [18]. In addition, an increase in the gas residence time (i.e., lower carrier gas flow rates) positively affected the yields of water and condensable organic compounds at the expense of the produced gas, probably as a result of a higher extent of both condensation and repolymerization reactions.

Regarding the yields of the main gaseous species released (i.e., CO_2, CO, H_2, and CH_4), some considerations can be drawn from the plot of the effects shown in Fig. A.3. The yield of CO_2 was greatly affected by pressure, which favored decarboxylation of both hemicelluloses and cellulose [17]. The yield of CO was positively affected by both the peak temperature and the presence of CO_2 in the carrier gas, probably as a result of the shift of the Boudouard reaction equilibrium towards CO production. An increased peak temperature also resulted in higher yields of hydrogen and methane, due to the higher extent of both the cracking and dehydrogenation reactions at temperatures higher than 500 °C [16]. Contrary to what was expected, an increased pressure did not result in any significant increase in y_{CH4}. This finding, which was also observed for wheat straw pellets [16], could be explained by the relatively narrow range of pressures applied in our study. For instance, Chen et al. [19] observed a marked increase in the yield of methane when pressure was raised above 1.0 MPa.

3.2. Properties of produced biochars

Table 3 reports the results of response variables related to potential stability (atomic H:C and O:C ratios, as well as the fixed-carbon content, x_{FC}), textural properties (S_{BET} and V_{ultra}), atomic C:N ratio, and pH. Fig. 2 displays the normal probability plots of the standardized effects for each response variable, whereas the regression coefficients of the statistical models are listed in Table A.3.

As can be seen in Fig. 2a, the fixed-carbon content was significantly improved by peak temperature, since its increase led to a higher aromatization of the biochar structure. The lower atomic H:C and O:C ratios measured for the biochars produced at the highest peak temperature confirmed their higher aromaticity (see Fig. 2b and c). The relatively high values of x_{FC} and low values of both the atomic H:C and O:C ratios for biochars produced at 550 °C highlight them as promising recalcitrant carbon sources for soil applications. In addition, Fig. 2d reveals that the absolute pressure was the most influential parameter on y_{FC}. The gas residence time and peak temperature also affected positively y_{FC}, albeit to a lesser extent. The highest fixed-carbon yield was 0.28, which is higher than that obtained for wheat straw pellets in the same range of operating conditions [16]. This can be due to the major content of lignin in the WW feedstock (28.9 vs 18.4 wt. %).

The peak temperature was by far the most influential factor on both the specific surface areas (S_{BET}) and ultra-micropore volumes (V_{ultra}) of

Table 2
Mass balance closures and experimental yields of pyrolysis products.

Factor					Response variable							
T	P	τ	CO2	Mass balance closure	y_{char}	y_{org}	y_{wat}	y_{gas}	y_{CO2}	y_{CO}	y_{CH4}	y_{H2}
° C	MPa	s	vol. %	%	mass fraction in dry basis				mol kg^{-1} in daf basis			
550	0.2	200	0	88.9	0.304	0.095	0.302	0.299	4.844	2.345	0.564	0.828
550	0.9	200	0	86.7	0.315	0.078	0.246	0.360	5.557	2.937	1.341	1.056
475	0.55	150	30	85.6	0.327	0.083	0.285	0.305	3.765	3.656	1.602	0.414
550	0.2	100	60	84.6	0.297	0.089	0.302	0.311	3.744	3.610	2.086	0.823
475	0.55	150	30	83.7	0.323	0.076	0.282	0.320	3.993	3.682	1.765	0.484
550	0.9	200	60	84.0	0.319	0.072	0.234	0.375	4.977	3.874	2.253	0.762
400	0.2	200	0	91.5	0.369	0.102	0.254	0.275	4.445	2.275	0.638	0.089
400	0.2	100	0	91.9	0.369	0.092	0.267	0.271	4.404	2.222	0.631	0.090
400	0.9	100	0	80.0	0.362	0.056	0.175	0.407	6.642	3.296	0.860	0.223
550	0.2	100	0	84.2	0.311	0.066	0.224	0.398	5.954	3.228	2.105	0.770
400	0.9	100	60	78.0	0.357	0.050	0.160	0.433	7.520	2.895	0.851	0.214
400	0.9	200	60	87.2	0.370	0.066	0.221	0.343	6.033	2.244	0.580	0.121
550	0.9	100	0	80.5	0.314	0.067	0.189	0.430	6.437	3.708	1.719	1.441
400	0.9	200	0	85.5	0.369	0.068	0.218	0.345	5.784	2.660	0.517	0.161
400	0.2	200	60	90.8	0.352	0.108	0.299	0.241	3.319	2.726	0.700	0.122
550	0.2	200	60	86.0	0.308	0.098	0.308	0.286	2.340	4.452	2.750	0.909
400	0.2	100	60	88.0	0.352	0.108	0.258	0.282	4.316	2.635	0.774	0.094
475	0.55	150	30	83.5	0.325	0.078	0.270	0.327	4.282	3.522	1.747	0.467
550	0.9	100	60	82.7	0.314	0.057	0.194	0.435	6.325	4.248	1.688	0.857

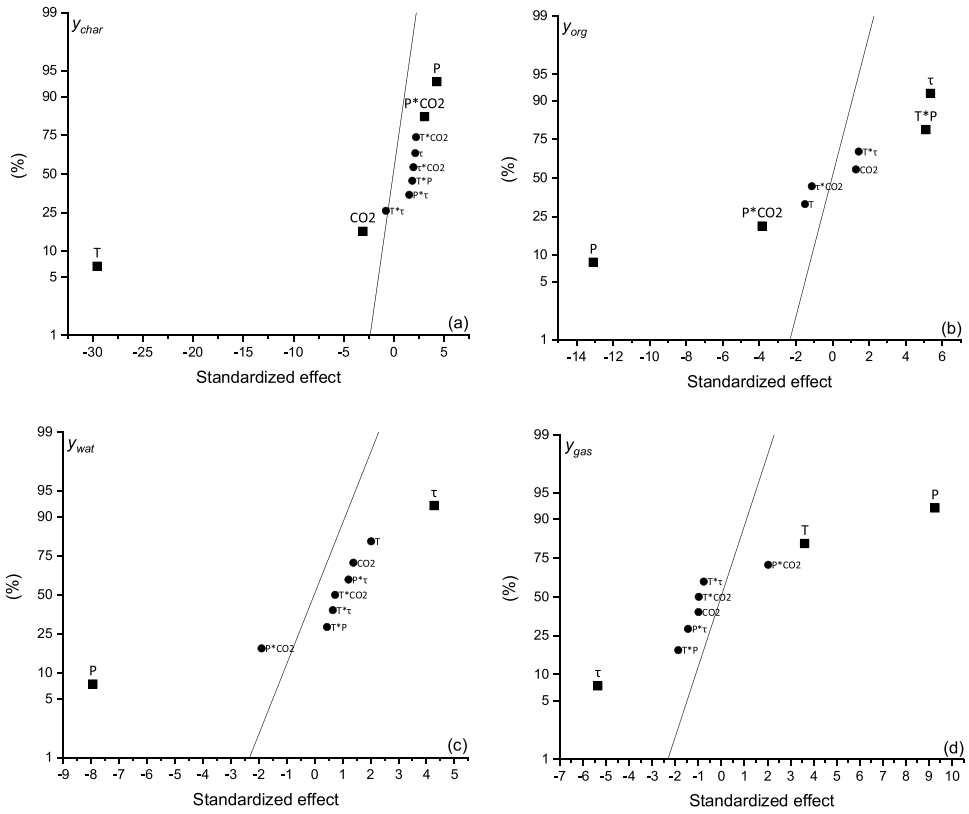

Fig. 1. Normal plot of the standardized effects (α = 0.05) for (a) y_{char}, (b) y_{org}, (c) y_{water}, and (d) y_{gas} (square, significant effect; circle, non-significant effect).

Table 3
Physicochemical properties of produced biochars (the subscript "w" refers to the results obtained for water-washed biochars).

Factor				Response variable								
T °C	*P* MPa	*τ* s	*CO2* vol. %	H:C –	O:C	C:N	*pH*	pH_w	x_{FC} *wt. %*	y_{FC} –	S_{BET} $m^2\ g^{-1}$	V_{ultra} $cm^3\ g^{-1}$
550	0.2	200	0	0.434	0.077	78.33	8.20	7.83	84.5	0.255	246	0.062
550	0.9	200	0	0.388	0.066	85.77	8.36	7.76	86.6	0.271	246	0.063
475	0.55	150	30	0.511	0.113	71.18	8.40	7.38	75.3	0.244	198	0.046
550	0.2	100	60	0.377	0.054	76.70	8.36	7.70	85.3	0.250	255	0.064
475	0.55	150	30	0.483	0.094	75.43	8.41	7.55	78.6	0.251	215	0.051
550	0.9	200	60	0.356	0.056	76.21	8.42	7.50	88.2	0.279	256	0.067
400	0.2	200	0	0.603	0.125	82.51	8.44	7.05	69.4	0.255	166	0.036
400	0.2	100	0	0.640	0.142	71.04	8.34	7.06	68.5	0.251	159	0.034
400	0.9	100	0	0.584	0.118	76.28	8.39	6.99	71.4	0.257	171	0.038
550	0.2	100	0	0.415	0.073	73.97	8.42	7.30	83.4	0.256	242	0.060
400	0.9	100	60	0.593	0.122	76.47	8.31	7.27	70.8	0.252	173	0.039
400	0.9	200	60	0.616	0.131	78.60	8.29	6.76	69.3	0.256	163	0.036
550	0.9	100	0	0.396	0.060	72.36	8.39	7.29	83.7	0.261	240	0.060
400	0.9	200	0	0.586	0.117	83.04	8.42	6.73	73.0	0.269	172	0.038
400	0.2	200	60	0.582	0.114	76.00	8.52	7.25	73.0	0.256	170	0.038
550	0.2	200	60	0.428	0.103	76.88	8.35	7.76	85.4	0.261	243	0.091
400	0.2	100	60	0.602	0.111	58.17	8.40	7.26	68.8	0.241	175	0.038
475	0.55	150	30	0.475	0.087	73.06	8.40	7.77	79.2	0.256	218	0.052
550	0.9	100	60	0.328	0.042	71.94	8.43	7.52	87.0	0.273	270	0.070

the resulting biochars (see the corresponding plots of the effects in Fig. A.4). Higher temperatures induced a more extended thermal degradation of biomass, resulting in the formation of new pores. At a much lesser extent than temperature, feeding CO_2 in the pyrolysis reactor also positively influenced the development of ultra-micropores, as a consequence of the above-mentioned slight gasification. On the other hand, it is important to note that the influence of the absolute pressure resulted to be negligible on the porosity development in the range of 0.2–0.9 MPa, in contrast to the negative effects that were reported in the literature [32,35]. This encouraging result suggests that pressurized pyrolysis at relatively low temperatures could be feasible for the production of engineered biochars with an ameliorated carbon sequestration potential without altering their porosity development.

From Table 3, it can be seen that biochars resulted to be moderately basic, since the values of pH were comprised between 8.20 and 8.52, which may indicate the availability of a certain level of both macro- and micro-nutrients [36], having been concentrated in the biochar matrix during the pyrolysis process. These pH values dropped down to 6.73–7.83 for water-washed biochars. This could be mainly ascribed to the loss of some water-soluble basic species (e.g., salts and minerals).

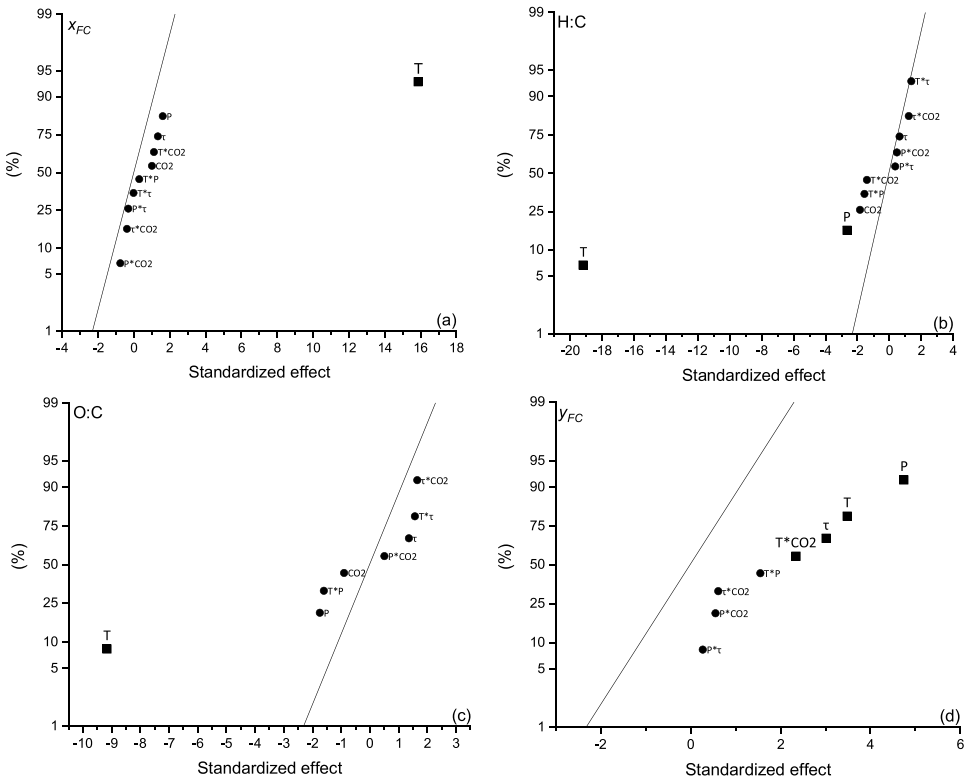

Fig. 2. Normal plots of the standardized effects (α = 0.05) for (a) x_{FC}, (b) atomic H:C ratio, (c) atomic O:C ratio, and (d) y_{FC} (square, significant effect; circle, non-significant effect).

From the normal plot of the effects shown in Fig. A.5a, it can be deduced a significant interaction effect between peak temperature and pressure, which results in an increase in pH at the highest levels of both factors. This finding could probably be due to an enhanced consumption of volatiles (which typically show an acidic nature [6]) through secondary reactions. By contrast, the interaction effect between the gas residence time and peak temperature led to lower values of pH, likely due to the major extent of recondensation reactions at longer vapor residence times.

On the other hand, the atomic C:N ratio was mainly (and positively) affected by the gas residence time (see the corresponding plot of the effects in Fig. A.5b), probably due to a higher release of nitrogen-containing volatile compounds. All the biochars produced in this study showed atomic C:N ratios much higher than the threshold value of 30, indicating their high suitability for the mitigation of N_2O emissions from soil [37,38].

3.3. PAHs contents in biochars

Table 4 lists the PAHs contents and TTEC values of produced biochars (the regression coefficients of the statistical models are reported in Table A.4). For its part, Fig. 3 shows the normal probability plots of the effects of the selected factors on the PAHs contents. As can be seen in Fig. 3a, an increase in either the peak temperature or the absolute pressure led to a marked decrease in the concentration of total PAHs. Within the available literature, no clear consensus exists on the influence of pyrolysis peak temperature on PAHs content in biochar. For instance, Kloss et al. [39] did not observe any correlation in the range of 400 − 525 °C for wheat straw, poplar wood, and spruce wood biochars; however, Rogovska et al. [40] reported an increase in the PAHs contents with temperature (in the range between 450 and 850 °C) for biochars obtained from hardwood, corn and switchgrass. Nevertheless, the studies by Brown et al. [9] and Freddo et al. [41] yielded the opposite trend at temperatures ranging from 300 to 1000 °C. To explain these apparently contradictory results, it is important to note that the total PAHs content takes into account all the processes involved in the formation and consumption of PAHs, which occurred at the solid-vapor interphase throughout different temperature phases in fast/slow succession until the peak temperature was reached [8]. In other words, PAHs may turn into lower molecular weight PAHs by breakage (which can subsequently be desorbed from the solid surface [42]) or into higher molecular weight PAHs through condensation and polymerization reactions [43,44]. Depending on the pyrolysis reactor configuration, operating process conditions and type of feedstock, different extents of the above-cited PAHs conversion pathways could be expected. In the present study, the highest PAHs content was reached at the lowest temperature level (400 °C), suggesting that conversion of PAH compounds toward lighter hydrocarbons was promoted by temperature.

At a first glance, the statistically significant negative effect of the absolute pressure on the total PAHs content could appear in disagreement with previous studies [45]. However, it might be explained by the relatively high carrier gas flow rates employed in order to ensure the proper gas residence time, which massively diluted the reaction environment, reducing the vapor-solid interaction and, consequently, preventing condensation and polymerization reactions and enhancing desorption of low-weight PAHs. Furthermore, a combined effect of the gas residence time and the presence of CO_2 in the carrier gas led to a slight increase in the total PAHs content. This appears to be in line with the findings reported in an earlier study [46].

The effects of factors on the contents of low-molecular weight PAHs (the sum of naphthalene, acenaphthylene, acenaphthene and fluorene contents, *PAH light* in Fig. 3b), medium-molecular weight PAHs (the sum of phenanthrene, anthracene and fluoranthene contents, *PAH medium* in Fig. 3c), and high-molecular weight PAHs (the sum of pyrene, benzo[a] anthracene and chrysene contents, *PAH heavy* in Fig. 3d) were also assessed. The criterion used to classify the PAH species in the three as-mentioned fractions was based on the number of aromatic rings in their structures, being this fact responsible for most of their

Table 4
16 EPA PAH contents and TTEC values for each biochar (see the Nomenclature section for abbreviations). "N.D." (not determined) refers to the PAH peaks visible but under quantification limit, whereas "n.d." (not detected) refers to those under the detection limit.

Factor				PAH content															
T	*P*	*τ*	*CO2*	*NAP*	*&%Annotation-xml.content;*	*ANA*	*FLU*	*PHE*	*ANT*	*FLT*	*PYR*	*BaA*	*CHR*	*BbF*	*BkF*	*BaP*	*IPY*	*DBA*	*BPE*	*Total*	*TTEC*
°C	MPa	s	vol. %	μg kg^{-1} biochar, db																	
550	0.2	200	0	2344	n.d.	599	110	298	58	85	95	12	18	n.d.	n.d.	n.d.	n.d.	n.d.	n.d.	3619	5.46
550	0.9	200	0	1901	n.d.	662	122	247	1034	70	46	N.D.	N.D.	n.d.	n.d.	n.d.	n.d.	n.d.	n.d.	4083	14.18
475	0.55	150	30	3245	n.d.	775	271	396	74	107	65	28	50	n.d.	n.d.	n.d.	n.d.	n.d.	n.d.	5010	8.85
550	0.2	100	60	2312	n.d.	787	179	477	110	114	72	N.D.	N.D.	n.d.	n.d.	n.d.	n.d.	n.d.	n.d.	4051	5.53
475	0.55	150	30	2714	n.d.	774	217	618	133	127	102	47	72	n.d.	n.d.	n.d.	n.d.	n.d.	n.d.	4804	11.33
550	0.9	200	60	1884	n.d.	632	149	296	110	75	50	n.d.	n.d.	n.d.	n.d.	n.d.	n.d.	n.d.	n.d.	3197	4.19
400	0.2	200	0	1543	388	656	219	1180	137	427	392	54	75	n.d.	n.d.	n.d.	n.d.	n.d.	n.d.	5071	12.37
400	0.2	100	0	1809	665	696	174	790	94	364	348	92	136	n.d.	n.d.	n.d.	n.d.	n.d.	n.d.	5168	16.38
400	0.9	100	0	2367	416	485	278	747	82	151	130	89	114	n.d.	n.d.	n.d.	n.d.	n.d.	n.d.	4860	15.45
550	0.2	100	0	3455	n.d.	598	127	410	66	128	70	10	22	n.d.	n.d.	n.d.	n.d.	n.d.	n.d.	4886	6.70
400	0.9	100	60	1972	n.d.	735	145	438	118	147	113	43	71	n.d.	n.d.	n.d.	n.d.	n.d.	n.d.	3782	9.76
400	0.9	200	60	2123	219	748	177	649	98	229	187	101	145	n.d.	n.d.	n.d.	n.d.	n.d.	n.d.	4677	16.90
550	0.9	100	0	1717	n.d.	764	182	415	150	74	104	N.D.	15	n.d.	n.d.	n.d.	n.d.	n.d.	n.d.	3421	5.19
400	0.9	200	0	1155	517	454	130	545	60	200	194	88	130	n.d.	n.d.	n.d.	n.d.	n.d.	n.d.	3474	13.91
400	0.2	200	60	2103	362	632	291	1092	341	304	298	66	93	n.d.	n.d.	n.d.	n.d.	n.d.	n.d.	5583	16.05
550	0.2	200	60	2380	n.d.	444	97	352	61	114	59	n.d.	14	n.d.	n.d.	n.d.	n.d.	n.d.	n.d.	3522	4.20
400	0.2	100	60	1677	646	603	159	731	109	219	211	57	72	n.d.	n.d.	n.d.	n.d.	n.d.	n.d.	4484	11.77
475	0.55	150	30	2464	n.d.	715	200	541	132	102	84	27	46	n.d.	n.d.	n.d.	n.d.	n.d.	n.d.	4310	8.60
550	0.9	100	60	1987	n.d.	440	220	298	307	70	59	n.d.	n.d.	n.d.	n.d.	n.d.	n.d.	n.d.	n.d.	3379	6.18

physicochemical properties [47]. It was observed that, among the three fractions, PAH light resulted to be the most affected by pressure, which seemed to promote further decomposition and desorption of PAH compounds and/or partly inhibit their formation. It is important to note that PAH light was the most abundant fraction in the produced biochars. On the other side, the operating parameter that mostly affected (negatively) both the PAH medium and PAH heavy groups was the peak temperature, whereas the effect of pressure was very low or even negligible for PAH medium and PAH heavy, respectively.

From the PAHs concentrations listed in Table 4, it can be seen that a highest value of 5583 μg kg^{-1} was measured for the biochar produced at 400 °C, 0.2 MPa and 200 s, while the lowest value (3197 μg kg^{-1}) corresponded to the biochar produced at 550 °C, 0.9 MPa and 100 s. In both cases, a CO_2-containing carries gas (60 vol. %) was used. From Table 4, it is also possible to observe that PAH compounds having ring structures more complex than chrysene were not detected for the range of operating conditions adopted in the present work. According to the European Biochar Certificate (EBC) guidelines [3], half of the produced biochars exceeded the limit concentration (4000 μg kg^{-1}) allowed for being considered as premium biochars. However, assuming the recommendations made by the International Biochar Initiative (IBI) [4], all the produced biochars can be marked as premium quality ones (i.e., PAHs content below 6000 μg kg^{-1}).

Concerning the TTEC values (which ranged from 4.19 to 16.9 μg kg^{-1}), the pyrolysis peak temperature was the most influential factor, leading to a marked decrease in this response variable when temperature was increased (see Fig. 3e). The effect of the absolute pressure was negligible in this case. These findings were perfectly in line with the considerations reported above, especially with those related to PAH medium and PAH heavy fractions, which represent the most toxic classes of PAHs.

The PAHs assessment was also conducted for water-washed biochars. As expected, the measured total PAHs contents (as well as those corresponding to the light, medium and heavy PAH fractions) were the same than those obtained for the unwashed biochars and, therefore, they are not reported herein.

3.4. Germination response

Once it has been ensured that the produced biochars had relatively low contents of hazardous PAH compounds, a germination assessment was performed to assess their short-term phytotoxicity. The germination index (calculated as in Eq. (1)) lower than 50 % indicates a high level of phytotoxicity, values comprised between 50 % and 80 % are representative of moderate phytotoxicity, whereas a lack of phytotoxicity is accomplished when *GI* falls between 80 % and 100 % [25]. Furthermore, the biochar could be defined as phytostimulant or phytonutrient when *GI* values exceed 100 %.

Table 5 shows the *GI* values obtained for the tested species (see Table A.5 for model regression coefficients). The germination response for barley was very sensitive to the pyrolysis operating conditions, showing a relatively wide response window: from low phytotoxicity (51.4 % as the lowest value) to moderate phytostimulation (up to 157 %). From Fig. 4a, it can be deduced a significant (and positive) interaction effect between peak temperature and pressure. The increase in *GI* when both factors were kept at their highest level could be explained by the relatively low contents of PAHs (as discussed above) as well as the higher extent of secondary reactions, which are promoted by either temperature or pressure and result in a higher consumption of volatile organic compounds. On the opposite side, the interaction effect between peak temperature and gas residence time on *GI* for barley was negative. This could be related to the higher contents of PAHs measured for biochars produced at the highest level of gas residence time.

Regarding the germination of watercress, the most part of the produced biochars resulted to be highly phytotoxic, regardless of the operating conditions adopted during pyrolysis (see Table 5). A possible

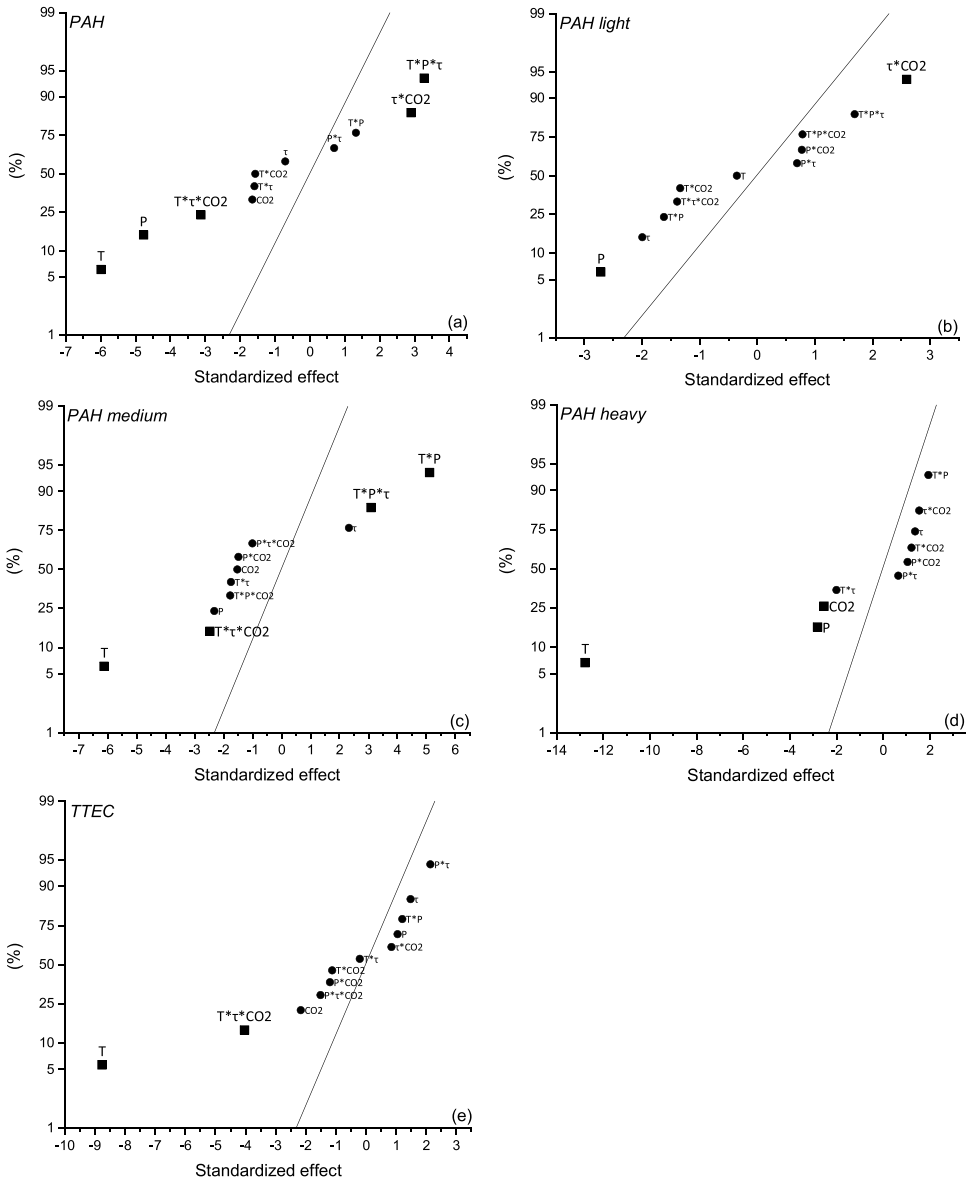

Fig. 3. Normal plots of the standardized effects (α = 0.05) for (a) total PAHs content, (b) low molecular weight PAHs content, (c) medium molecular weight PAHs content, (d) high molecular weight PAHs content, and (e) TTEC (square, significant effect; circle, non-significant effect).

reason behind this could be the high sensitivity of watercress to the biochar ash content, which can cause salt stress in the plant [48]. As can be seen in Fig. 4b, an increased peak temperature resulted in lower *GI* values, whereas the absolute pressure had a positive effect on the germination response.

For basil, germination resulted to be the less sensitive to the different pyrolysis conditions. In fact, no significant effects were detected for any of the main or 2-way interaction effects assessed, as shown in Fig. 4c. The observed variability in the *GI* values (from 61.0% to 139.5%) was then mainly explained by factors outside the regression model.

As can also be observed from the data reported in Table 4, the levels of phytotoxicity were noticeably reduced after washing the biochars, especially in the case of watercress, for which outstanding values of *GI* (up to 228.8 %) were measured. An improvement in the germination behavior was also observed for barley. However, the effect of washing biochar on the germination response of basil was unclear (i.e., no evident trend can be deduced). Results from the germination assessment seem to suggest that PAHs were not the only ones responsible for the short-term phytotoxic effects related to biochars. In fact, and as suggested by Buss et al. [49], the co-occurrence of low-molecular weight organic acids and phenolic compounds, which have high mobility and can be removed relatively easily by water washing, could partly explain the above-mentioned phytotoxic effects of biochars. In any case, the water washing pretreatment for wood waste-derived biochars appears to be a highly useful and low-cost means of diminishing their potential toxicity for soil application purposes.

4. Conclusions

Some useful considerations can be drawn from the results shown and discussed above:

- The total PAHs content in the produced biochars can be significantly reduced by increasing either the peak temperature or the absolute pressure (ideally both). The extent of PAHs volatilization could be promoted at higher temperatures, while an increased pressure (at high flow rates of carrier gas) could partly inhibit repolymerization and recondensation reactions (which lead to PAHs formation). Generally speaking, the resulting wood waste-derived biochars were

Table 5
GI values for watercress, barley, and basil. The subscript "w" refers to the results obtained when washed biochars were tested.

Factor				Germination index (*GI*)					
T °C	*P* MPa	*τ* s	*CO2* vol. %	*GI barley* %	*GI watercress*	*GI basil*	GI_w *barley*	GI_w *watercress*	GI_w *basil*
550	0.2	200	0	98.50	24.76	118.6	157.9	129.7	99.80
550	0.9	200	0	90.39	42.21	91.56	143.0	115.1	75.56
475	0.55	150	30	103.0	36.18	93.80	185.2	124.2	77.15
550	0.2	100	60	74.77	43.06	105.8	212.3	85.28	170. 4
475	0.55	150	30	75.38	14.82	139.5	100.8	155.8	86.37
550	0.9	200	60	62.76	50.97	78.61	41.36	86.79	81.97
400	0.2	200	0	134.5	44.08	62.79	91.93	165.7	95.13
400	0.2	100	0	90.09	46.85	121.0	57.21	228.8	136.7
400	0.9	100	0	51.35	50.99	117.6	99.09	183.8	85.25
550	0.2	100	0	87.39	35.59	77.21	117.8	99.07	144.1
400	0.9	100	60	68.47	58.11	103.1	143.5	90.15	141.6
400	0.9	200	60	69.07	67.49	100.4	136.8	198.5	122.2
550	0.9	100	0	78.08	41.49	61.03	196.9	203.0	126.5
400	0.9	200	0	101.8	69.60	73.76	66.32	121.9	78.02
400	0.2	200	60	136.0	48.04	104.8	144.1	105.0	72.39
550	0.2	200	60	75.08	29.64	74.72	222.8	180.5	53.94
400	0.2	100	60	83.78	49.68	118.6	39.72	100.6	110.8
475	0.55	150	30	70.57	32.60	111.7	84.76	72.07	161.0
550	0.9	100	60	157.1	64.98	99.27	104.2	79.37	79.35

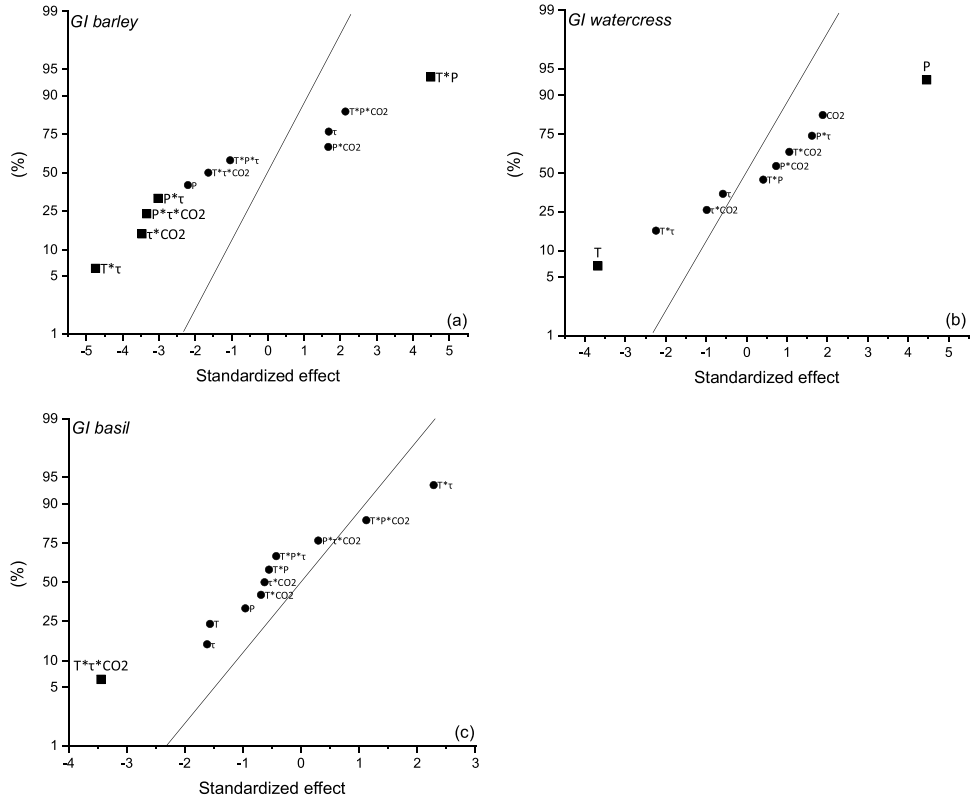

Fig. 4. Normal plots of standardized effects (α = 0.05) for the germination index (*GI*) of (a) barley, (b) watercress, and (c) basil (square, significant effect; circle, non-significant effect).

of good quality in terms of PAH hazard, making them suitable for soil amendment purposes.

- The phytotoxic or phytostimulant effect of wood waste-derived biochar depended mainly on the process pyrolysis conditions as well as the seed species considered for the germination essay. In any case, germination indices notably increased (in some cases from phytoxic to phytostimulant responses) when biochars were washed with water before being tested. This suggests that the acute phytotoxicity observed for some biochars can be ascribed to water-soluble acidic and phenolic compounds.
- From an applied research point of view, pressurized slow pyrolysis (at a moderate peak temperature of 550 °C and relatively high carrier gas flow rates) followed by an inexpensive water washing step appears as an interesting pathway to produce premium-quality and value-added biochars from wood waste.

CRediT authorship contribution statement

Gianluca Greco: Conceptualization, Methodology, Software, Validation, Formal analysis, Investigation, Data curation, Writing - original

draft. **María Videgain:** Data curation, Methodology, Investigation, Resources. **Christian Di Stasi:** Data curation, Methodology, Investigation, Resources. **Elisabet Pires:** Data curation, Methodology, Software, Validation, Investigation, Resources, Writing - review & editing, Supervision. **Joan J. Manyà:** Resources, Writing - review & editing, Visualization, Supervision, Project administration.

Declaration of Competing Interest

The authors declare that they have no known competing financial interests or personal relationships that could have appeared to influence the work reported in this paper.

Acknowledgements

This project has received funding from the European Union's Horizon 2020 research and innovation program under the Marie Skłodowska-Curie grant agreement No 721991. JJM and EP also acknowledge the funding from the Aragón Government (Refs. T22_20R and E37_20R, respectively), co-funded by FEDER 2014-2020 "Construyendo Europa desde Aragón". EP acknowledges the Spanish Ministerio de Ciencia, Innovación y Universidades (project number RTI2018-093431-B-I00). The authors gratefully thank the ISQCH Chromatography Service, José Antonio Manso and Eugenio Vispe Palacín for their help in the preparation and characterization of the samples.

Appendix A. Supplementary data

Supplementary material related to this article can be found, in the online version, at doi:https://doi.org/10.1016/j.jaap.2021.105337.

References

[1] S. Chandra, J. Bhattacharya, Influence of temperature and duration of pyrolysis on the property heterogeneity of rice straw biochar and optimization of pyrolysis conditions for its application in soils, J. Clean. Prod. 215 (2019) 1123–1139, https://doi.org/10.1016/j.jclepro.2019.01.079.

[2] European Commission Regulation (ECR) No 1881/2006, Setting Maximum Levels for Certain Contaminants in Foodstuffs, 2006. https://eur-lex.europa.eu/homepage.html.

[3] European Biochar Certificate (EBC), European Biochar Certificate – Guidelines for a Sustainable Production of Biochar, Arbaz, Switzerland, 2019, https://www.european-biochar.org/biochar/media/doc/ebc-guidelines.pdf.

[4] IBI, Standardized Product Definition and Product Testing Guidelines for Biochar that is Used in Soil, 2015. https://biochar-international.org/.

[5] H.P. Schmidt, I. Hilber, T.D. Bucheli, Polycyclic aromatic hydrocarbons and polychlorinated aromatic compounds in biochar. Biochar Environ. Manag., 2nd edition, Routledge, London, 2015, p. 30.

[6] C. Wang, Y. Wang, H.M.S.K. Herath, Polycyclic aromatic hydrocarbons (PAHs) in biochar – their formation, occurrence and analysis: a review, Org. Geochem. 114 (2017) 1–11, https://doi.org/10.1016/j.orggeochem.2017.09.001.

[7] D. Fabbri, A.G. Rombolà, C. Torri, K.A. Spokas, Determination of polycyclic aromatic hydrocarbons in biochar and biochar amended soil, J. Anal. Appl. Pyrolysis 103 (2013) 60–67, https://doi.org/10.1016/j.jaap.2012.10.003.

[8] W. Buss, M.C. Graham, G. MacKinnon, O. Mašek, Strategies for producing biochars with minimum PAH contamination, J. Anal. Appl. Pyrolysis 119 (2016) 24–30, https://doi.org/10.1016/j.jaap.2016.04.001.

[9] R.A. Brown, A.K. Kercher, T.H. Nguyen, D.C. Nagle, W.P. Ball, Production and characterization of synthetic wood chars for use as surrogates for natural sorbents, Org. Geochem. 37 (2006) 321–333, https://doi.org/10.1016/j.orggeochem.2005.10.008.

[10] S.E. Hale, J. Lehmann, D. Rutherford, A.R. Zimmerman, R.T. Bachmann, V. Shitumbanuma, A. O'Toole, K.L. Sundqvist, H.P.H. Arp, G. Cornelissen, Quantifying the total and bioavailable polycyclic aromatic hydrocarbons and dioxins in biochars, Environ. Sci. Technol. 46 (2012) 2830–2838, https://doi.org/10.1021/es203984k.

[11] B.R.T. Simoneit, Biomarker PAHs in the environment. PAHs Relat. Compd. Handb. Environ. Chem. (Anthropogenic Compd.), Springer, Berlin, Heidelberg, 1998, https://doi.org/10.1007/978-3-540-49697-7_5.

[12] J.M. De la Rosa, H. Knicker, E. López-Capel, D.A.C. Manning, J.A. González-Perez, F.J. González-Vila, Direct detection of black carbon in soils by Py-GC/MS, carbon-13 NMR spectroscopy and thermogravimetric techniques, Soil Sci. Soc. Am. J. 72 (2008) 258–267, https://doi.org/10.2136/sssaj2007.0031.

[13] M.J. Antal, S.G. Allen, X. Dai, B. Shimizu, M.S. Tam, M. Gronli, Attainment of the theoretical yield of carbon from biomass, Ind. Eng. Chem. Res. 39 (2000) 4024–4031, https://doi.org/10.1021/ie000511u.

[14] J. Madej, I. Hilber, T.D. Bucheli, P. Oleszczuk, Biochars with low polycyclic aromatic hydrocarbon concentrations achievable by pyrolysis under high carrier gas flows irrespective of oxygen content or feedstock, J. Anal. Appl. Pyrolysis 122 (2016) 365–369, https://doi.org/10.1016/j.jaap.2016.09.005.

[15] G. Greco, M. Videgain, C. Di Stasi, B. González, J.J. Manyà, Evolution of the mass-loss rate during atmospheric and pressurized slow pyrolysis of wheat straw in a bench-scale reactor, J. Anal. Appl. Pyrolysis 136 (2018) 18–26, https://doi.org/10.1016/j.jaap.2018.11.007.

[16] G. Greco, C. Di Stasi, F. Rego, B. González, J.J. Manyà, Effects of slow-pyrolysis conditions on the products yields and properties and on exergy efficiency: a comprehensive assessment for wheat straw, Appl. Energy 279 (2020), 115842, https://doi.org/10.1016/j.apenergy.2020.115842.

[17] Y. Qian, J. Zhang, J. Wang, Pressurized pyrolysis of rice husk in an inert gas sweeping fixed-bed reactor with a focus on bio-oil deoxygenation, Bioresour. Technol. 174 (2014) 95–102, https://doi.org/10.1016/j.biortech.2014.10.012.

[18] F. Ates, N. Miskolczi, B. Saricaoglu, Pressurized pyrolysis of dried distillers grains with solubles and canola seed press cake in a fixed-bed reactor, Bioresour. Technol. 177 (2015) 149–158, https://doi.org/10.1016/j.biortech.2014.10.163.

[19] Y. Chen, L. Zhang, Y. Zhang, A. Li, Pressurized pyrolysis of sewage sludge: process performance and products characterization, J. Anal. Appl. Pyrolysis 139 (2019) 205–212, https://doi.org/10.1016/j.jaap.2019.02.007.

[20] M. Azuara, E. Sáiz, J.A. Manso, F.J. García-Ramos, J.J. Manyà, Study on the effects of using a carbon dioxide atmosphere on the properties of vine shoots-derived biochar, J. Anal. Appl. Pyrolysis 124 (2017) 719–725, https://doi.org/10.1016/j.jaap.2016.11.022.

[21] U. Mantau, Wood Flows in Europe (EU 27), Proj. Report, Comm. by CEPI (Confederation Eur. Pap. Ind.) CEI-Bois (European Confed. Woodwork. Ind.), 2012.

[22] G. Faraca, A. Boldrin, T. Astrup, Resource quality of wood waste: the importance of physical and chemical impurities in wood waste for recycling, Waste Manage. 87 (2019) 135–147, https://doi.org/10.1016/j.wasman.2019.02.005.

[23] J.M. De la Rosa, Á.M. Sánchez-Martín, P. Campos, A.Z. Miller, Effect of pyrolysis conditions on the total contents of polycyclic aromatic hydrocarbons in biochars produced from organic residues: assessment of their hazard potential, Sci. Total Environ. 667 (2019) 578–585, https://doi.org/10.1016/j.scitotenv.2019.02.421.

[24] N.-D. Dat, M.B. Chang, Review on characteristics of PAHs in atmosphere, anthropogenic sources and control technologies, Sci. Total Environ. 609 (2017) 682–693, https://doi.org/10.1016/j.scitotenv.2017.07.204.

[25] C. Liang, G. Gascó, S. Fu, A. Méndez, J. Paz-Ferreiro, Biochar from pruning residues as a soil amendment: effects of pyrolysis temperature and particle size, Soil Tillage Res. 164 (2016) 3–10, https://doi.org/10.1016/j.still.2015.10.002.

[26] D.C. Montgomery, Design and Analysis of Experiments, 6th edition, John Wiley & Sons, New York, 2005.

[27] A.I. Moreno, R. Font, Pyrolysis of furniture wood waste: decomposition and gases evolved, J. Anal. Appl. Pyrolysis. 113 (2015) 464–473, https://doi.org/10.1016/J.JAAP.2015.03.008.

[28] H.J. Gehrmann, H. Mätzing, P. Nowak, D. Baris, H. Seifert, C. Dupont, F. Defoort, M. Peyrot, F. Castagno, Waste wood characterization and combustion behaviour in pilot lab scale, J. Energy Inst. 93 (2020) 1634–1641, https://doi.org/10.1016/J.JOEI.2020.02.001.

[29] C. Di Blasi, G. Signorelli, C. Di Russo, G. Rea, Product distribution from pyrolysis of wood and agricultural residues, Ind. Eng. Chem. Res. 38 (1999) 2216–2224, https://doi.org/10.1021/ie980711u.

[30] L. Zhao, X. Cao, O. Mašek, A. Zimmerman, Heterogeneity of biochar properties as a function of feedstock sources and production temperatures, J. Hazard. Mater. 256–257 (2013) 1–9, https://doi.org/10.1016/j.jhazmat.2013.04.015.

[31] A.V. McBeath, C.M. Wurster, M.I. Bird, Influence of feedstock properties and pyrolysis conditions on biochar carbon stability as determined by hydrogen pyrolysis, Biomass Bioenergy 73 (2015) 155–173, https://doi.org/10.1016/j.biombioe.2014.12.022.

[32] F. Melligan, R. Auccaise, E.H. Novotny, J.J. Leahy, M.H.B. Hayes, W. Kwapinski, Pressurised pyrolysis of Miscanthus using a fixed bed reactor, Bioresour. Technol. 102 (2011) 3466–3470, https://doi.org/10.1016/j.biortech.2010.10.129.

[33] J.J. Manyà, F.X. Roca, J.F. Perales, TGA study examining the effect of pressure and peak temperature on biochar yield during pyrolysis of two-phase olive mill waste, J. Anal. Appl. Pyrolysis 103 (2013) 86–95, https://doi.org/10.1016/j.jaap.2012.10.006.

[34] J.J. Manyà, S. Laguarta, M.A. Ortigosa, J.A. Manso, Biochar from slow pyrolysis of two-phase olive mill waste: effect of pressure and peak temperature on its potential stability, Energy Fuels 28 (2014) 3271–3280, https://doi.org/10.1021/ef500654t.

[35] E. Cetin, B. Moghtaderi, R. Gupta, T. Wall, Influence of pyrolysis conditions on the structure and gasification reactivity of biomass chars, Fuel 83 (2004) 2139–2150, https://doi.org/10.1016/J.FUEL.2004.05.008.

[36] L. Bouqbis, S. Daoud, H.W. Koyro, C.I. Kammann, F.Z. Ainlhout, M.C. Harrouni, Phytotoxic effects of argan shell biochar on salad and barley germination, Agric. Nat. Resour. 51 (2017) 247–252, https://doi.org/10.1016/j.anres.2017.04.001.

[37] M.L. Cayuela, L. van Zwieten, B.P. Singh, S. Jeffery, A. Roig, M.A. Sánchez-Monedero, Biochar's role in mitigating soil nitrous oxide emissions: a review and meta-analysis, Agric. Ecosyst. Environ. 191 (2014) 5–16, https://doi.org/10.1016/j.agee.2013.10.009.

[38] P. Brassard, S. Godbout, V. Raghavan, Soil biochar amendment as a climate change mitigation tool: key parameters and mechanisms involved, J. Environ. Manage. 181 (2016) 484–497, https://doi.org/10.1016/j.jenvman.2016.06.063.

[39] S. Kloss, F. Zehetner, A. Dellantonio, R. Hamid, F. Ottner, V. Liedtke, M. Schwanninger, M.H. Gerzabek, G. Soja, Characterization of slow pyrolysis biochars: effects of feedstocks and pyrolysis temperature on biochar properties, J. Environ. Qual. 41 (2012) 990–1000, https://doi.org/10.2134/jeq2011.0070.

[40] N. Rogovska, D. Laird, R.M. Cruse, S. Trabue, E. Heaton, Germination tests for assessing biochar quality, J. Environ. Qual. 41 (2012) 1014–1022, https://doi.org/10.2134/jeq2011.0103.
[41] A. Freddo, C. Cai, B.J. Reid, Environmental contextualisation of potential toxic elements and polycyclic aromatic hydrocarbons in biochar, Environ. Pollut. 171 (2012) 18–24, https://doi.org/10.1016/j.envpol.2012.07.009.
[42] T. McGrath, R. Sharma, M. Hajaligol, An experimental investigation into the formation of polycyclic-aromatic hydrocarbons (PAH) from pyrolysis of biomass materials, Fuel 80 (2001) 1787–1797, https://doi.org/10.1016/S0016-2361(01)00062-X.
[43] M. Keiluweit, M. Kleber, M.A. Sparrow, B.R.T. Simoneit, F.G. Prahl, Solvent-extractable polycyclic aromatic hydrocarbons in biochar: influence of pyrolysis temperature and feedstock, Environ. Sci. Technol. 46 (2012) 9333–9341, https://doi.org/10.1021/es302125k.
[44] R.K. Sharma, M.R. Hajaligol, Effect of pyrolysis conditions on the formation of polycyclic aromatic hydrocarbons (PAHs) from polyphenolic compounds, J. Anal. Appl. Pyrolysis 66 (2003) 123–144, https://doi.org/10.1016/S0165-2370(02)00109-2.
[45] T. Matamba, A. Tahmasebi, S. Khoshk Rish, J. Yu, Promotion effects of pressure on polycyclic aromatic hydrocarbons and H2 formation during flash pyrolysis of palm kernel shell, Energy Fuels 34 (2020) 3346–3356, https://doi.org/10.1021/acs.energyfuels.9b04409.
[46] Q. Chang, R. Gao, H. Li, G. Yu, F. Wang, Effect of CO2 on the characteristics of soot derived from coal rapid pyrolysis, Combust. Flame 197 (2018) 328–339, https://doi.org/10.1016/j.combustflame.2018.05.033.
[47] C. Achten, J.T. Andersson, Overview of polycyclic aromatic compounds (PAC), Polycyclic Aromat. Compd. 35 (2015) 177–186, https://doi.org/10.1080/10406638.2014.994071.
[48] W. Buss, O. Mašek, Mobile organic compounds in biochar – a potential source ofcontamination – phytotoxic effects on cress seed (Lepidiumsativum) germination, J. Environ. Manage. 137 (2014) 111–119, https://doi.org/10.1016/j.jenvman.2014.01.045.
[49] W. Buss, O. Mašek, M. Graham, D. Wüst, Inherent organic compounds in biochar-their content, composition and potential toxic effects, J. Environ. Manage. 156 (2015) 150–157, https://doi.org/10.1016/j.jenvman.2015.03.035.